12

DEC 23 1997

ESO-TP-73D
Jan 1997

Results of studies on the environmental factors affecting the VLTI performance.

B. Koehler, S. Levêque, O. von der Lühe,

European Southern Observatory,
Karl-Schwarzschild Strasse 2,
D-85748 Garching

ESO-TP-73D

ABSTRACT

In the last few years, we have undertaken a number of studies and experiments to assess the impact of various environmental factors on the performance of the ESO Very Large Telescope Interferometer (VLTI)[1]. The investigated topics include atmospheric turbulence, wind loads on the telescope structure, vibrations created by equipment, natural thermal variation, thermal load from electronics, natural and man-made seismic noise, as well as acoustic noise.

A first report of this activity was given in a previous paper[2]. This paper presents the final results obtained in 1995.

The main outcome is the very good confidence that the VLT 8m telescope and the infrastructure design is adequate for interferometric use at optical wavelengths down to the visible.

Keywords: Interferometry, optical aperture synthesis, performance, environment, seeing, thermal effects, vibrations, wind load, seismic, acoustic.

INTRODUCTION

Combining the VLT 8-m Unit Telescopes (UT) for aperture synthesis in the visible is undoubtedly a very challenging task for a number of reasons. First, the size and complexity of the telescope is a priori not favourable to the high dynamic stability required by interferometry. Secondly, the telescope has also to be optimised for other observing modes which have sometimes conflicting requirements with interferometry. Last but not least, experience with interferometric combination of such large telescopes does not exist yet anywhere in the world; most of presently operating stellar interferometers use apertures below one meter, the biggest one being the 1.5m apertures of GI2T[3].

The above considerations call for a thorough system engineering approach in order to keep the technical risk to an acceptable level. An element of this approach is the top-down generation and bottom-up validation of exhaustive error budgets for each major performance characteristic of the interferometer which is required by the science objectives. This process is illustrated on figure 1 and constitutes the framework of the activities reported here. The effects of environmental factors play an important role in these error budgets and need to be carefully evaluated as part of the performance verification process. Therefore we have invested, over the last few years, a significant effort in engineering studies of environmental effects, whose goals was:

(i) to better understand the effects of the environment on the interferometer performance,
(ii) to check that these effects can be maintained at a level compatible with the top-level requirements, and
(iii) to specify, when necessary, various sub-system requirements and operational constraints aiming at reducing them.

A first description of this activity together with preliminary results were given in a previous paper[2]. It will be referred to as paper n°1 in the following. The present paper reports on the final results obtained during 1995.

1. WIND LOAD EFFECTS

The investigations related to wind load effects were already described in paper n°1, with an emphasis on the analysis of the OPD stability inside the 8-m telescopes. The final results presented here-after are the outcome of an update of the same analysis performed with the final design of the telescope structure[4] and of the M1 cell/M3 tower[5]. The updated FEM is shown in figure 2. The main difference is the evolution of the center piece design which is now a more massive and stiffer box structure. This has resulted in a 8% increase of the total drag force. An other significant difference is the global

Fermilab Library
0 1160 0064852 1

improvement of the structure stiffness. All together, the deformation of the structure under wind load has significantly decreased.

The static OPD under a static 10 m/sec wind speed amounts to 5 µm instead of the previous 8.8 µm. This improvement is also noticeable on the dynamic results presented in figure 3 and in table 1. This table shows the results on the *OPD criterion* defined as the root mean square of the OPD variation (σ_T) over various exposure times (T) corresponding to observation at different wavelengths. The requirements are achieved even with the enclosure fully open (i.e. slit open without wind screen, louvers open and bottom ventilation door open). When the bottom ventilation door of the enclosure is closed, the results leave comfortable margin to account for the limited accuracy of this type of complex FEM analysis. First validation of the assumptions and of the FE model could be recently performed[4]. The harmonic response of the Top Unit measured on the pre-erected structure in Milan could be compared with that delivered by the FE model. A satisfactory fit has been obtained and confirmed, in particular, the adequacy of the damping factor of 0.75% conservatively assumed for this specific OPD analysis. A second positive validation was also obtained by comparing the wind spectra used in the analysis with the results of new wind tunnel tests performed in 1995.

In conclusion, the confidence that the 8-m telescope design is adequate for interferometry at visible wavelengths for outside wind speed up to at least 10 m/sec with fully open enclosure is very high. Optimisation of the enclosure configuration within the framework of the VLT Operational Model[6] remains to be investigated and may result in the possibility to observe at even higher wind speeds.

Observing wavelength (µm)		0.6	2.2	10
Exposure time T (msec)		10	48	290
Requirement on OPD criterion σ_T (nm)		*14*	*50*	*225*
OPD criterion (nm)	Enclosure fully open	**12**	**49**	**168**
	Bottom ventilation door closed	**9**	**38**	**100**

Table 1: OPD stability at the coudé focus of the UT under wind load (10 m/sec outside wind speed).

2. VIBRATION OF EQUIPMENT ON THE TELESCOPE

Several types of vibration-generating equipment which are attached to the telescope structure and could degrade the OPD stability have been identified. These include the ventilating fans and the liquid cooling system of electronics cabinets, as well as the close-cycle-cooler units used by VLT IR instruments. In these units which are expected to be running even during interferometric observation, both the cold head and the compressor are important sources of vibrations which can be transmitted to the telescope structure. The cold head will be attached to the instrument vessel and the compressor will be installed on the Nasmyth platform.

The detailed FEM of the telescope shown on figure 2 has been used to investigate these effects and to derive requirements for the decoupling devices to be inserted between the equipment and the telescope structure. The computation method, similar to the one used for the wind and seismic loads, consists of computing the harmonic response of the complete telescope structure to a unitary stimulus -a single force in that case-. The OPD harmonic response is then computed from the displacement of each mirror using a sensitivity matrix. The Power Spectral Density (PSD) of the OPD is then computed from the PSD of the disturbance force and the OPD harmonic response. In order to simulate the effect of the decoupling devices and to specify their stiffness and damping characteristics, the transfer function of a second order with given resonance frequency and damping factor is also included.

Figures 4 and 5 show the disturbance force spectra measured in ESO laboratory on prototypes of the ISAAC[7] cold head and compressor. The cold head features a 2Hz fundamental vibration with all its harmonics. This is the result of the periodic shocks of the displacer against its mechanical limits, in spite of its built-in damper. The compressor disturbance dominates around 45 Hz corresponding to its fundamental rotation frequency.
Figures 6 and 7 plot the resulting OPD criterion for visible wavelength as a function of the resonance frequency of the decoupling device. It can be deduced from these plots that decoupling devices with frequencies below 5 Hz are necessary to maintain the OPD variation inside the telescope below a few nanometers. These curves also evidence the high

disturbance level which can result from a bad selection of the characteristics of the decoupling devices. As an example, a decoupling frequency of 6 Hz for the cold head would result in 50 nm OPD variation and up to 10 μm r.m.s. can result from a 40 Hz decoupling frequency associated with a poor damping. A similar analysis has been performed for the image motion. Decoupling frequencies below 5 Hz ensure image motion at the milli-arcsecond level but frequencies around 10 Hz can already result in 0.1 arcsec image jitter. These requirements have been implemented in the design of the IR instruments.

3. SEEING EFFECTS

A number of VLTI-specific studies related to *external seeing* and *internal seeing* effects have already been reported in paper n°1.

As far as external seeing is concerned, data from balloon-borne probes launched from Paranal during the PARSCA campaign[8] were used to compute the PSD of the atmospheric tilt disturbance, and the variance of the differential OPD due to anisoplanatic effects. This last topic has been further investigated in order to generate an error budget for the field of view performance of VLTI. The data from PARSCA campaign were used to compute the PSD of the differential OPD in a given field and for various conditions of seeing, baseline and telescope diameter. Figure 8 shows typical results obtained from a given measured profile best representative of the median conditions at Paranal ($r_0 \approx 21$ cm, $t_0 \approx 10$ msec at 0.6 μm). The spatial averaging effect resulting from the aperture size is clearly visible. These data have been used to assess the visibility loss due to OPD anisoplanatism when using an off-axis star for co-phasing the interferometer. This effect has to be added to the visibility loss due to the various on-axis error sources which already amount to ≈40% for observation at 2.2μm. Accepting a further 20% visibility loss for OPD anisoplanatism, the field limitation for off-axis co-phasing in the median seeing conditions amounts to ≈10 arcsec at 2.2 μm and ≈40 arcsec at 10 μm.

Concerning *internal seeing* effects, the measurements of lateral beam wander presented in paper n°1 were complemented with measurements of OPD fluctuations due to air turbulence along long propagation path. The same underground tunnel of the Technical University of Munich which is fairly well representative of the delay line tunnel at Paranal was used. The goals of these measurements were: (i) to assess the applicability of Kolmogorov laws in this type of conditions, and (ii) to validate the anticipated level of OPD fluctuation due to air turbulence inside the light ducts and the delay line tunnel assumed in our error budgets. A commercial laser interferometer was used to measure the optical path along one beam propagating over 10 to 120 meters as well as the OPD between two parallel beams, some centimeters apart, propagating over similar distances. A detailed report of these measurements can be found elsewhere[9]. A typical result is shown in figure 9 where the PSD of the OPD fluctuation for a 20m propagation path is presented. It evidences significant deviation from Kolmogorov laws. Fluctuations above 10 Hz are dominated by the noise of the laser interferometer but they remain inside the error budget (5 nm RMS over 10 msec for a 120m path). The variance of the fluctuations due to air turbulence, when translated into an equivalent Cn^2, corresponds to values from below 10^{-14}. This gives confidence that our target of $Cn^2 = 10^{-15}$ can be reached inside the light ducts and delay line tunnel where the thermal environment is expected to be better (see also section 4).

4. THERMAL EFFECTS

It was decided at an early stage of the project, to place the delay lines and the beam transport optics inside air-filled light ducts and tunnel, as opposed to vacuum pipes. This choice, motivated by cost reasons, has a number of consequences among which are the necessity to correct for longitudinal dispersion effects[10], and to ensure a proper thermal environment in order to avoid significant air turbulence and thermal gradients.

To address this last point belonging to environmental factors, an extensive thermal study has been undertaken. A detailed description of the goals, the method and assumptions of that study together with preliminary results have been given in paper n°1. We will report here on the final results obtained after optimisation of the insulation design as well as on the last part of the study concerning the impact of artificial (man-made) heat sources. We will also report on the attempt made to predict the three dimensional distribution of the Cn^2 inside the delay line tunnel with and without artificial heat sources.

First results from a 3D model including the central part of the delay line tunnel and the interferometric laboratory triggered a slight modification of the tunnel insulation in its central part. A fairly good thermal homogeneity could be reached in this central area. A more serious problem was encountered in the area of the Auxiliary Telescope Stations. Indeed, the lack of insulation around the station concrete block embedded in the ground as well as thermal bridges inside the station cover were the origin of temperature differences of the order of 2°C along the light ducts. This led us to include a 100 mm thick insulation layer all around the station and to improve the lid design. A summary of the results is given in table 2.

• dT/dz (vertical gradient)	±0.2 °C/m
• ΔT (longitudinal homogeneity)	< 0.5 °C over the entire underground facilities < 0.2 °C in the entire laboratory + central tunnel volume
• Daily temperature variation	<= 0.02 °C
• Seasonal temperature variation	± 2.4 °C inside the light ducts ± 2.0 °C inside the delay line tunnel and laboratory

Table 2: Final results of the simulated thermal environment inside the VLTI underground facilities.

A second part of the study focused on the impact of artificial thermal loads. The first load cases intended to simulate the heat created during maintenance periods inside the tunnel. The goal was to check that the above performance could be restored after a reasonable recovery time. The dominating heat source during maintenance is the lighting system consisting of 100 W lamps located on the tunnel ceiling. Both convective (25%) and radiative (75%) power was modelled. Several types of maintenance cycles were computed, ranging from long occasional maintenance period (1w of continuous activity with required recovery time < 1 day) to repeated short periods (1 h every day without deterioration of the above performance).
The short term effect of the lighting on the pre-existing vertical gradient was found to be a negative contribution, i.e. towards instability. This is explained by the fact that the radiative part of the heat input is absorbed by the tunnel floor whose temperature raises slightly, creating therefore potentially unstable conditions. On the other hand, the medium-to-long term effect, after the lighting has been switch off, was found to be a positive contribution to the vertical gradient. This, in turn, is explained by the progressive temperature increase in the vicinity of the lamps through conduction/convection mechanisms. For long maintenance periods, the maximum negative gradient at the end of the lighting period could reach -0.25°C/m. But in all cases, the contribution to the gradient after the specified recovery time was found to be within the range ± 0.05 °C/m, well within the acceptable values.
Another disturbance to be expected after maintenance activity is the air motion created by the movement of people. This can create significant air turbulence for some time. especially when a stable gradient pre-exists. This effect can be seen on laboratory experiments and has indeed been observed in operating stellar interferometers. To limit its impact, we have included a thin removable partition wall between the interferometric laboratory (where the most frequent human presence is expected) and the delay line tunnel.

A second set of artificial load cases concerned the impact of heat dissipated by equipment located inside the tunnel. For that purpose, four heat sources, representative of typical electronic boxes installed on the Delay Line carriage, were located in the middle of a 70m-long section in a 3D model of the tunnel. The boxes were assumed to dissipate purely convective power ranging from -10W (over-cooled) to 50 W (under-cooled). After computation of the temperature distribution inside the tunnel using a 3D thermal model, a volume difference "k-ε" type of turbulence modelling tool was used to compute the 3D air flow pattern inside the tunnel. Figure 10 shows an example of the results for the mean air velocity for the 50 W case. Maximum velocities of 0.2 m/sec are reached in the plumes developing right above each heat source.

In order to relate these results more directly to the optical performance, the 3D distribution of refractive index structure coefficient (Cn^2) was then computed from the kinetic energy (k), the dissipation rate of turbulent energy (ε), and the temperature variance using semi-empirical relations[11,12]. Figure 11 illustrates the results. It shows the iso-contours of the Cn^2 averaged along the tunnel length. It shall be noted that the relations mentioned above use empirical coefficients derived for the near-ground atmospheric turbulence. Their applicability to our case is uncertain. Also, for simplification, the delay line structure has not been included in the model. This calls for a cautious interpretation of the Cn^2 values which should be considered as orders of magnitude.

Nevertheless, we can conclude from this analysis that the target level of $Cn^2 < 10^{-15}\ m^{-2/3}$ averaged along the light beams appears to be achievable with some margin in the absence of disturbance and with reasonable confidence as long as the heat sources inside the tunnel are limited to about 15 W per delay line.

5. MICROSEISMIC EFFECTS

Seismic noise is obviously a prime concern for any interferometric experiment. The ground vibration, by exciting the structural resonances of the optics supports easily generate unacceptable OPD fluctuation which spoil the fringe contrast. As for most of the other environmental factors, we can distinguish between the *natural* seismic noise and the *artificial* (or man-made) ground motion created by human activity and vibration-generating equipment. Ensuring a low level of microseismic noise has been a concern since day one and has dictated many concept and design choices such as placing the Control Building off the Observatory Platform, placing the telescope hydraulic pumps on very efficient dampers, etc. Over the last years, we have paid constant attention to the various disturbance sources and we have tried, whenever possible, to evaluated quantitatively their impact on the VLTI performance. A general discussion of the microseismic effects, the rationale of the related engineering activities undertaken, an overview of the anticipated noise sources, as well as first results were presented in paper n° 1 as well as in a first article[13] published in the ESO review: *The Messenger*. We will focus, in the following, on the results of the microseismic measurement campaign performed at Paranal in March 1994. For a more detailed report, the reader shall refer to a second *Messenger* article[14].

A 10-days measurement campaign was carried out in March 1994 at Paranal in collaboration with the Institut de Physique du Globe (IPG), Strasbourg , France. The goal was to characterise the natural micro-seismicity at Paranal by: (i) measuring the natural *background seismic noise* in the absence of any seismic event and any artificial vibration source, (ii) characterising the intensity and recurrence of the *micro seismic activity*. In addition, the opportunity was taken to characterise some artificial vibration sources which can only be assessed by in-situ measurements, such as car driving on the access road and people walking on the Observatory platform. The measurement set-up included high sensitivity seismometers (Kinemetrics SS-1 and MarkProduct L4) associated with acquisition electronics (Reftek). The seismometers were installed on firm rock and buried at least 40 cm below the surface to avoid contamination by external disturbance such as wind buffeting.

The spectrum of the natural background noise is shown on figure 12. The level of ground acceleration above 1 Hz is extremely low (<10 ng/$\sqrt{Hz}$), well below that of other very quite sites known to us. It is indeed limited by the noise of the high-sensitivity seismometers. This is the direct consequence of the remoteness of the site. The ground motion was found indeed to be dominated by the impact of ocean waves observed at the low frequencies. This phenomenon is not shown in figure 12 but is included in table 3. A more detailed discussion can be found elsewhere[14].

On the other hand, a high seismic activity was recorded. The automatic acquisition chain was triggered on average every 20 minutes by a seismic event. For each event, the following parameters were calculated: (i) the distance of the earthquake epicenter from Paranal, (ii) the seismic moment, (iii) the Richter magnitude (ML) and (iv) a parameter representing the level of the local ground acceleration called Γ. This last parameter was defined in order to characterise each event in terms of its impact on the VLT structural deformation. From the observation that the PSD of the ground acceleration is basically flat (white noise) above 10 Hz and from the fact that the most relevant structural modes of the telescope structure are in that same frequency range, we defined Γ as the average level of the ground acceleration PSD in the frequency range [10-50 Hz] expressed in nano-g/$\sqrt{Hz}$. The smallest Γ value recorded was 6 ng/$\sqrt{Hz}$ corresponding to an earthquake of ML = 1.6 at 138 km. The largest value recorded was 9.581 µg/$\sqrt{Hz}$ corresponding to an earthquake of ML = 4.5 at 160 km. This last event occurred during the night and the acceleration was enough to awake several people at Paranal.
An example of a typical ground acceleration spectrum is shown on figure 12 for an event with Γ=510 ng/$\sqrt{Hz}$. The micro seismic activity relevant for the VLTI could then be characterised by extracting from the data the statistical relation between the parameter Γ and its frequency of occurrence. This "Γ-frequency" relation is shown on figure 13. It represents, as a function of Γ, the number of events for which the value Γ is exceeded during a given time window (here 125 hours, the total monitoring time). A fairly good linear fit is obtained in logarithmic scale. It shall be noted that the departure from the fit for low Γ values is due to the incompleteness of the data set for very small events which did not always trigger the acquisition.

The next step in the analysis was to compute the dynamic response of the 8-m telescope structure to a set of typical events. Table 3 presents the results for the event whose spectrum is shown in figure 12. For this type of event, which occurs in average 3 times per night, the required OPD stability is exceeded for observation in the visible and NIR.

Observing wavelength (μm)		0.6	2.2	10
Exposure time T (msec)		10	48	290
Requirement on OPD criterion σ_T (nm)		*14*	*50*	*225*
OPD criterion (nm)	natural background noise	**3**	**12**	**72**
	during seismic event s850336, (Γ=510 ng/$\sqrt{Hz}$)	**64**	**109**	**119**

Table 3: OPD stability at the Coudé focus of the UT under natural background seismic noise (no artificial disturbance, no seismic event) and for a typical micro earthquake occurring 3 times per night on average.

We can then determine, for each wavelength, the Γ threshold above which the specification is exceeded. From the "Γ-frequency" law, we can then infer the corresponding period of recurrence. The result is shown in the table 4 below.

Observing wavelength (μm)	0.6	2.2	10
Exposure time (msec)	10	48	290
Disturbing threshold Γ_0 (ng/$\sqrt{Hz}$)	110	234	964
Period of recurrence of disturbing events	**40 min.**	**1 h 40 min.**	**8 h**

Table 4: Periods of recurrence of seismic events for which the OPD stability specified for the UT is reached.

For events larger than the above thresholds, the performance of the interferometer will be degraded for about 1 minute, the typical duration of micro-earthquakes as observed during the field measurements. Assuming that the data collected during the event are corrupted and cannot be used, this corresponds to a loss of observing time of 1 min./40 min. =2.5 % in the worst case (observation in the visible). Another way to consider these results is to compute the probability to exceed the Γ-thresholds in a given observing time window. The statistical processing of the collected data show, for example, that during an observation of 10 min., the probability to exceed the disturbing threshold in the visible (0.6μm), NIR (2.2μm) and TIR (10μm) is respectively ≈ 20%, 8% and 2%.

These results evidence an important impact of the seismic activity at Paranal on the VLTI performance. The immediate consequence is the need to monitor the seismic activity at the site during VLTI operation with the 8m telescopes. For this purpose, a seismic monitoring system has been included in the Astronomical Site Monitor of the VLT. It will consist of several seismometers monitoring the ground acceleration on the site. They will inform the VLTI Control System of the occurrence of any significant seismic events to allow immediate action to be taken (e.g., close the instrument shutter in the case of long exposures) and will store in a data base the recorded ground accelerations to be used during post-processing (e.g., for identification of corrupted snap-shot exposures).
A second consequence can be drawn from this study. The major part of the OPD variation energy over short exposures appears to originate from the excitation of local axial modes of the support of mirrors M5, M6 & M8 in the Coudé train of the 8m telescope and not from global modes of the telescope structure. This means that an improvement of the results presented here may be expected after optimisation of these Coudé mirror supports during their final design.
The third consequence concerns a metrology system based on laser interferometer and accelerometers which could be developed to monitor in real time the OPD variations inside the telescope in view of their correction with the PZT-mounted secondary mirror of the Delay Lines. Even though the studies of other disturbances reported in this article have shown that such a metrology is not essential, it remains the subject of one of our on-going research & development activities, and provisions have been included in the telescope design for its possible implementation.
As a final remark, we can state that the early knowledge of the results of such a detailed analysis would not have impaired the selection of Paranal as the VLT/VLTI site. Indeed, the max. 2.5% loss in observing time due to microseismic activity remains negligible with regards to the gain (up to 200 %) brought by the improved seeing and cloud conditions which was identified during the VLT site selection process[15].

6. ACOUSTIC EFFECTS

Even though acoustic noise effects are not a real concern for most interferometric experiments in the laboratory, they have been considered one of the important environmental factors to be looked at in some details for the VLTI. Indeed, the very large area of the VLT 8-m mirror as well as the overlapping of the eigen-frequency ranges of the mirror support, the enclosure structure and the enclosure acoustic cavity led us to undertake a detailed study aiming at evaluating the OPD fluctuation due to acoustic noise in the VLT enclosure. Two major acoustic sources can be identified: (i) the vortices created by the interaction of the wind with the entrance slit and, (ii) equipment located inside the enclosure and running during observation. In this last category, the close-cycle-coolers of the IR instruments were identified as major sources.

A description of the study goals, method and preliminary results have been given in paper n° 1. We will just recall here that the study is based on an elasto-acoustic computer model of the VLT primary mirror inside the enclosure using the RAYON software. RAYON is a general software package for vibro-acoustics which solves axisymetric and 3D complex problems involving coupled structures and fluids. We will report here on the second phase of the study whose goal was to quantitatively estimate the mirror response to the major acoustic sources.

A measurement campaign was undertaken in November 1994 to measure the acoustic noise generated by the wind vortices attached to the edges of the enclosure slit. For that purpose, the 3.6m and the NTT enclosures at La Silla were selected as best representative candidates. Six highly sensitive microphones were placed along both sides of the entrance slit and two were placed close to the telescope. Measurements were made for several wind incidence angles with respect to the slit and for various wind speeds. The measured pressure spectra were then used to infer a representative acoustic source model. Two source models were investigated leading to very similar results, one consisting of incoming plane waves and a second consisting of 6 acoustic dipoles attached to the slit. The pressure measurement close to the telescope were also used to check the accuracy of the acoustic modelling by comparing them to the simulated results obtained from an acoustic model of the 3.6m dome specially built for that purpose using the same RAYON software. Satisfactory agreement (within 6 dB) was obtained after adjustment of the enclosure acoustic absorption to a value corresponding to a reverberant time of 4 s. These source models and acoustic absorption were then input to the 3D VLT elasto-acoustic model (see figure 14) to compute the mirror response in terms of average axial motion ("piston") as well as higher Zernike modes. The results of "piston" OPD stability are presented in table 5 for a 10 m/sec incoming wind speed. The amplitude of the higher Zernike modes remains negligible (<6 nm r.m.s. for long exposure times). The PSD of "piston" OPD shown in figure 15 evidences a main contribution coming from the first axial eigenmode of the mirror in its cell, around 13 Hz.

Observing wavelength (μm)	0.6	2.2	10
Exposure time T (msec)	10	48	290
Requirement on OPD criterion σ_T (nm)	*14*	*50*	*225*
OPD criterion (nm)	**9.9**	**37.2**	**42.1**

Table 5: OPD fluctuation due to acoustic noise inside the VLT enclosure generated by the interaction of the wind with the entrance slit. Incoming wind speed: 10 m/sec. Wind incidence angle: 0°.

For what concerns acoustic noise generated by equipment, the spectrum of acoustic noise power was measured in the laboratory for both the cold head and the compressor prototypes of the ISAAC close-cycle-cooler. The results were then input in the 3D VLT model in the form of acoustic monopoles at the respective locations. The resulting OPD was found to remain negligible, about 10 times below the requirement, even without the foreseen acoustic shield around the equipment.

In spite of the care taken in validating the model and in using measured acoustic inputs, the accuracy of this type of study remains somewhat uncertain. Nevertheless, we can conclude that acoustic noise effects cannot be neglected but should remain within acceptable limits. Attention to them shall be kept during the commissioning phase.

7. CONCLUSION

A number of studies related to environmental factors have allowed us to *define* or *refine specifications* for several VLT/VLTI subsystems particularly critical for the VLTI operation. This has concerned, among others, the tunnel insulation, the heat dissipation inside the tunnel, the first axial eigenfrequency of the M2 unit, the stiffness of the Coudé

mirror supports, the vibration-decoupling devices of the instrument close-cycle-coolers, and the need for seismic monitoring.

The results obtained have *confirmed that the performance requirements set for the VLTI are achievable*. They have shown that the design of the VLT Observatory and, in particular, the 8m Unit Telescopes is compatible with the stringent requirements imposed by visible interferometric observations.

The decisive confirmation of this conclusion on the real hardware has already started and will continue as hardware becomes available and commissioned on the site.

8. ACKNOWLEDGEMENTS

We wish to acknowledge the contributions of the various companies who participated in these studies, under ESO contract. We are also grateful to those ESO colleagues who spent some of their precious time in discussions providing valuable inputs, in particular F. Koch who prepared all FEM data used in the various models and helped in the critical interpretation of the results, J.L. Lizon who performed the vibration measurements on the close-cycle-coolers, and L. D'Arcio who, as a short term student at ESO, derived the formulae and developed the software tool to compute the quantities related to OPD anisoplanatism

9. REFERENCES

[1] O. von der Lühe et al., "Interferometry with the ESO Very Large Telescope", *in these proceedings.*

[2] B. Koehler et al., "Engineering aspects of environmental factors in VLTI", *Amplitude and Intensity Spatial Interferometry II*, J. Breckinridge (Ed.), in Proc. SPIE Vol. 2200, pp. 180-194, Kona 1994.(Paper n°1)

[3] F. Vakili et al., "Spectrally resolved interferometry with the Grand Interféromètre à 2 Télescopes: results and prospects", *Amplitude and Intensity Spatial Interferometry II*, J.B. Breckinridge (Ed.), in Proc. SPIE Vol. 2200, pp 216-221, Kona 1994.

[4] M. Quattri et al., "VLT 8-m Unit Telescope Main Structure", *in these proceedings.*

[5] S. Stanghellini et al., "Design and Construction of the VLT Primary Mirror Cell -Support of the large, thin primary mirror-", *in these proceedings.*

[6] V. Bäumer et al., "Operational model for VLT temperature and flow control", *in these proceedings.*

[7] A.F.M. Moorwood, " ISAAC -an Infrared Spectrometer and Array Camera for the ESO VLT", *in these proceedings.*

[8] M. Sarazin, "Site Atmospheric Characterisation", *Topical Meeting on Adaptive Optics*, M. Cullum (Ed.), in ESO Conference and Workshop Proc. N°54, pp 439-444, Garching bei München 1995.

[9] S. Levêque et al., "Measurement of optical path fluctuations due to internal seeing for the VLTI", *Advanced Imaging Technologies and Commercial Applications*, N. Clark (Ed.), in Proc. SPIE Vol. 2566, pp 156-163, San Diego 1995.

[10] S. Levêque et al., "Longitudinal Dispersion Compensation for the VLTI", accepted for publication in *Experimental Astronomy*, Kluwer academic publishers, March 1996.

[11] A.F. Baas et al., "The temperature structure function for complex terrain", *Eighth Symposium on Turbulent Shear Flows*, Technical University of Munich, 1991.

[12] J.C. Wyngaard et al., "Behavior of the refractive-Index-Structure Parameter near the Ground", JOSA, Vol. 61, N. 12, Dec. 1971, pp 1646-1650

[13] B. Koehler, "Hunting the Bad Vibes at Paranal!", *The Messenger* N°76 (June 1994), pp 4-9, 1994.

[14] B. Koehler et al., "Impact of the Microseismic Activity on the VLT Interferometer", *The Messenger* N°79 (March 1995), pp 4-9, 1995.

[15] M. Sarazin (Ed.), "VLT Site Selection Working Group, Final Report", *VLT Report N° 62*, ESO, 1990.

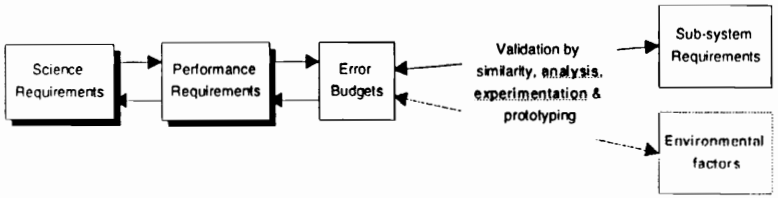

Figure 1: The requirement flow chart illustrating the need to address the effects of environmental factors as part of the validation of the top-level error budgets.

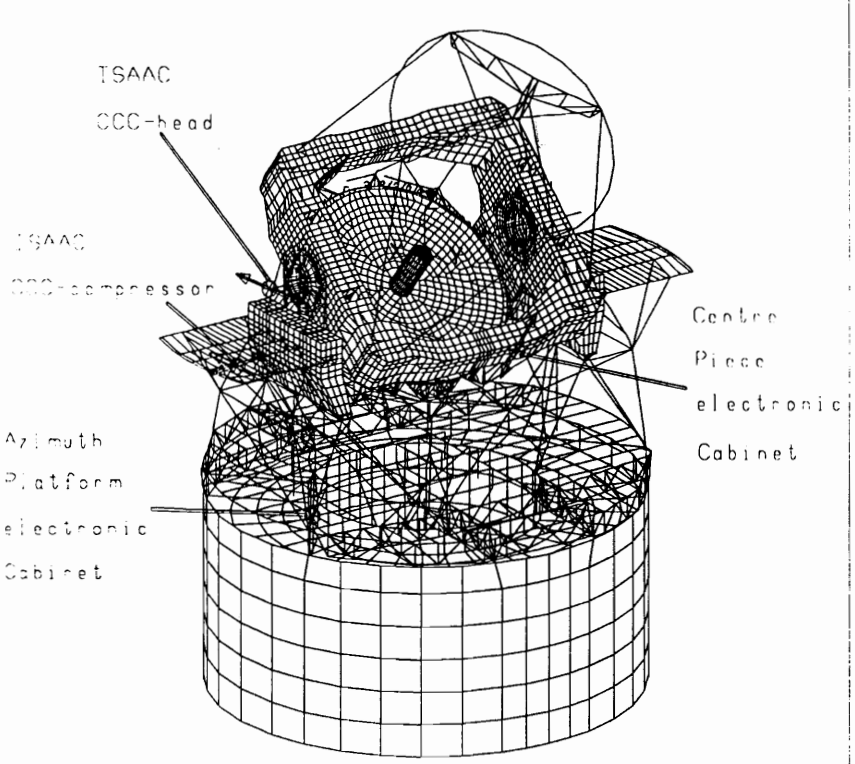

Figure 2: FEM of the VLT 8-meter Telescope used to evaluate the Optical Path Length Stability under dynamic wind load, seismic motion, and vibrating equipment.

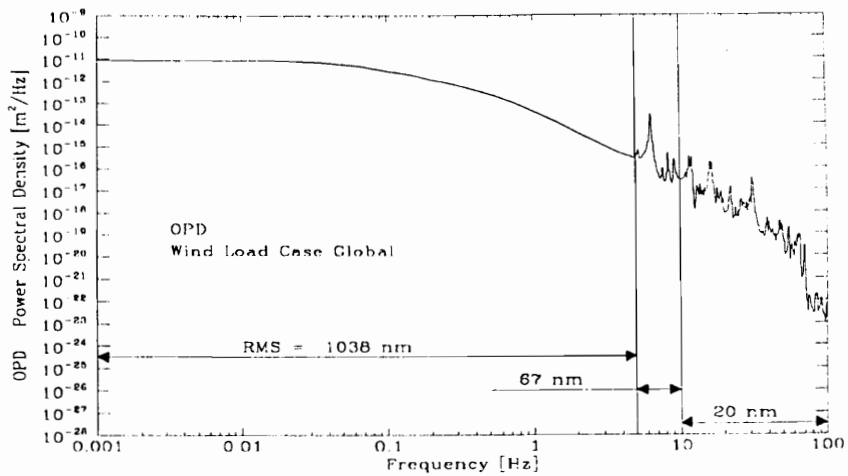

Figure 3: PSD of the OPD at the UT coudé focus under dynamic wind load (10 m/sec)

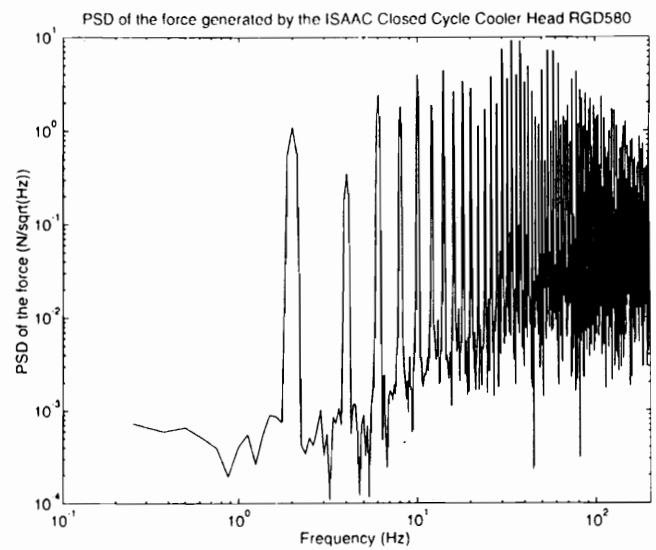

Figure 4: PSD of the disturbance force generated by the cold head of a close-cycle-cooler.

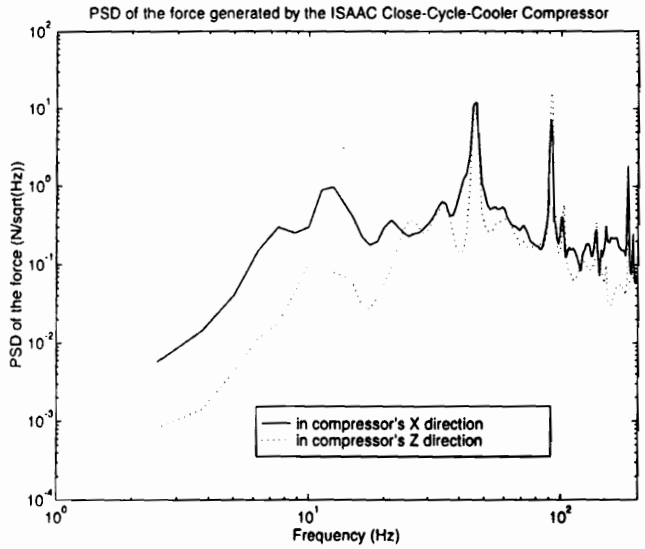

Figure 5: PSD of the disturbance force generated by the compressor of a close-cycle-cooler.

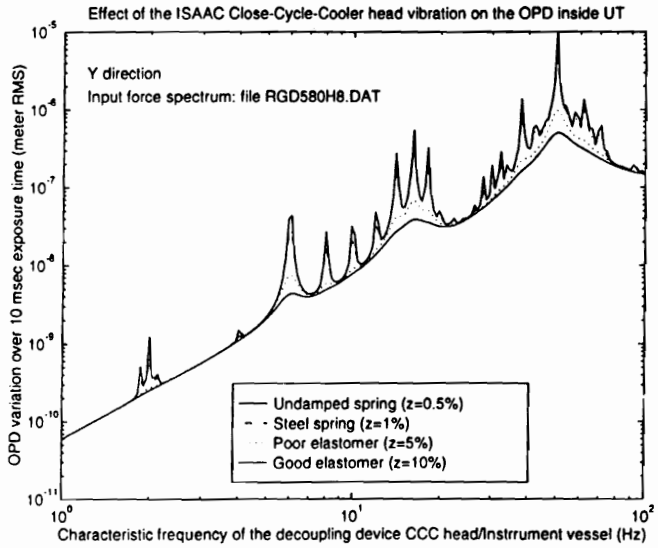

Figure 6: Effect of the vibration of the close-cycle-cooler heads of IR instrument on the OPD stability inside the 8-meter telescope.

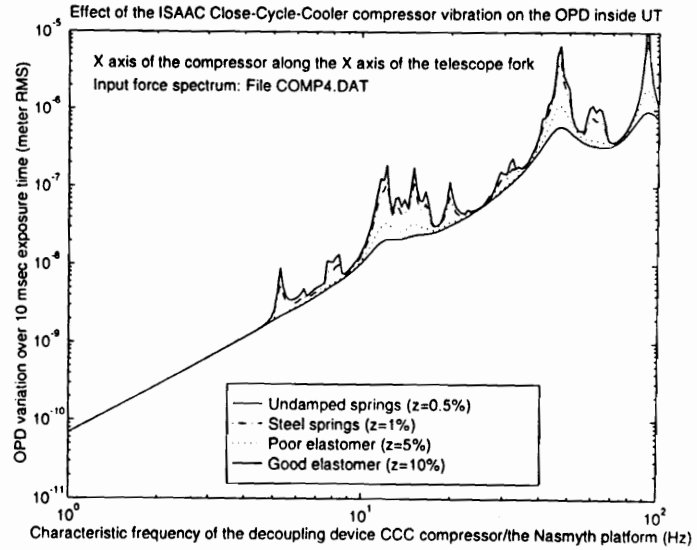

Figure 7: Effect of the vibration of the close-cycle-cooler compressor of IR instrument on the OPD stability inside the 8-meter telescope.

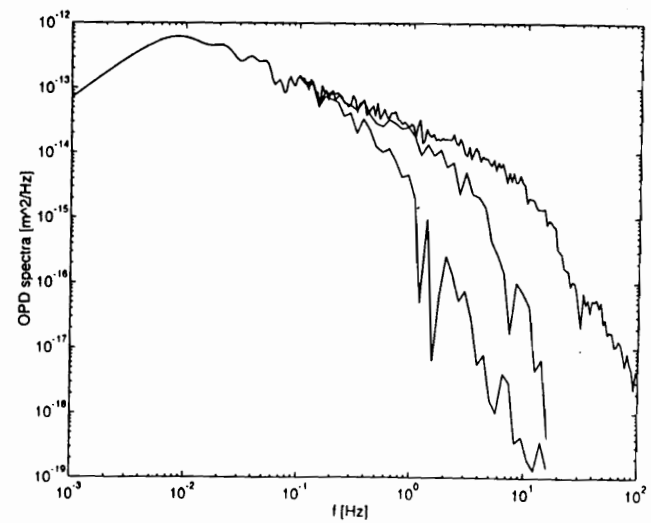

Figure 8: PSD of anisoplanatic OPD error at Paranal for a 210m baseline, 8 arcsec field separation and different apertures: *upper:* sub-r0 aperture, *middle:* 1.8m (AT), *lower:* 8m (UT)

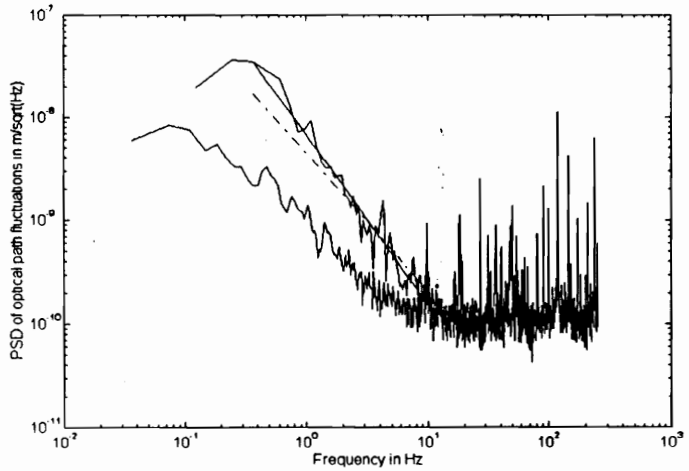

Figure 9: PSD of the Optical Path fluctuation inside a long underground tunnel representative of the Delay Line Tunnel.,*upper:* over a 20m path, *lower:* measurement noise, *Straight line (solid):* least square fit (slope -11/3), *Straight line (dashed):* slope -8/3

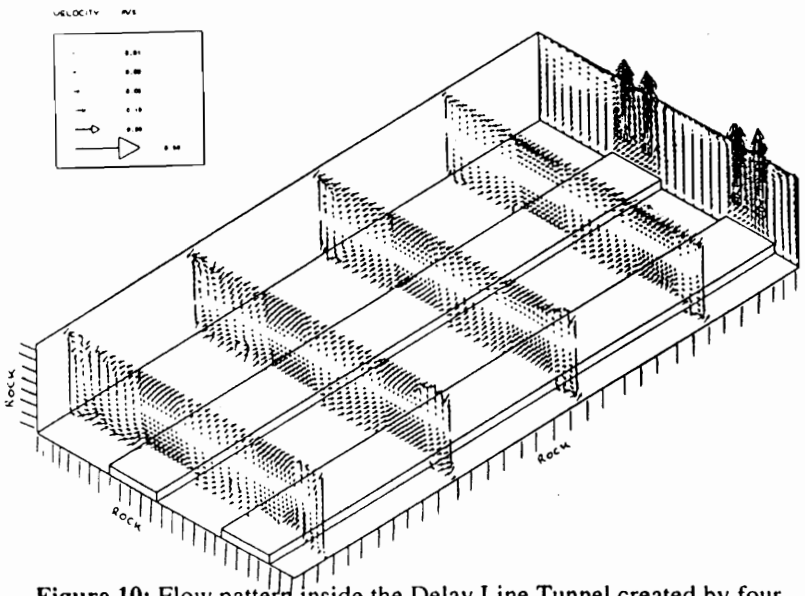

Figure 10: Flow pattern inside the Delay Line Tunnel created by four pieces of equipment dissipating 50 W each. The arrows represent the mean air velocity.

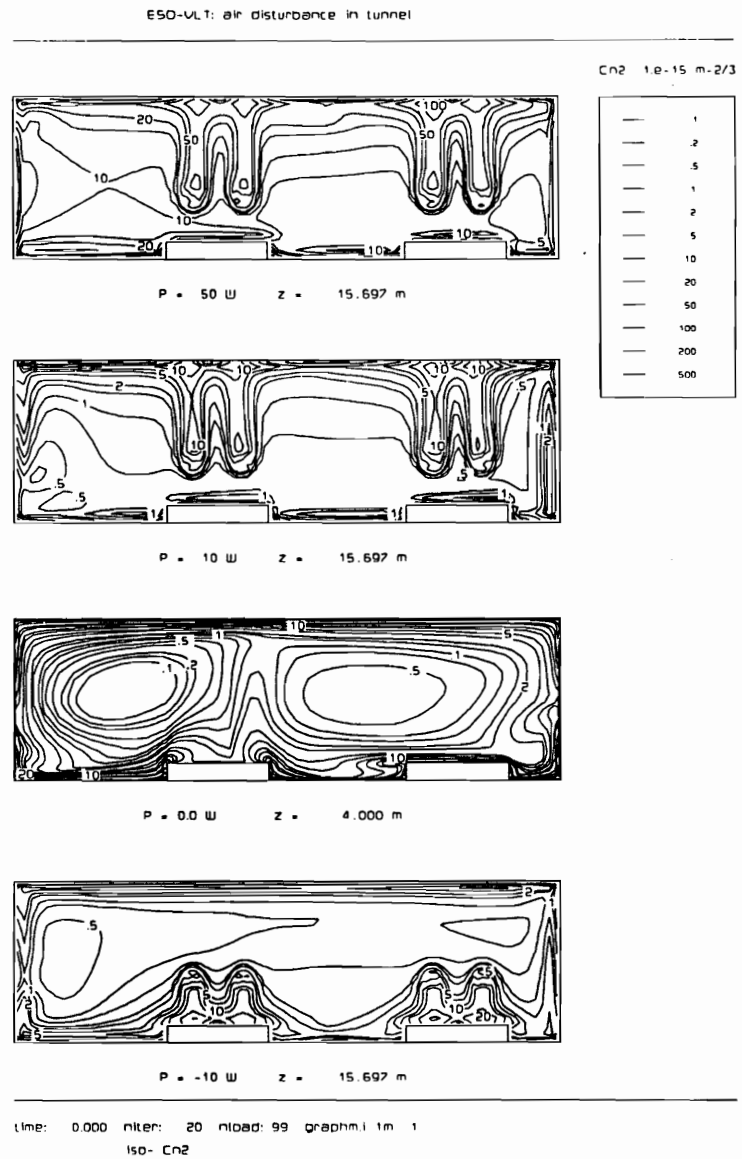

Figure 11: Iso-contour of Cn^2 averaged along the light path inside the tunnel for various cases of power dissipated by electronic boxes.

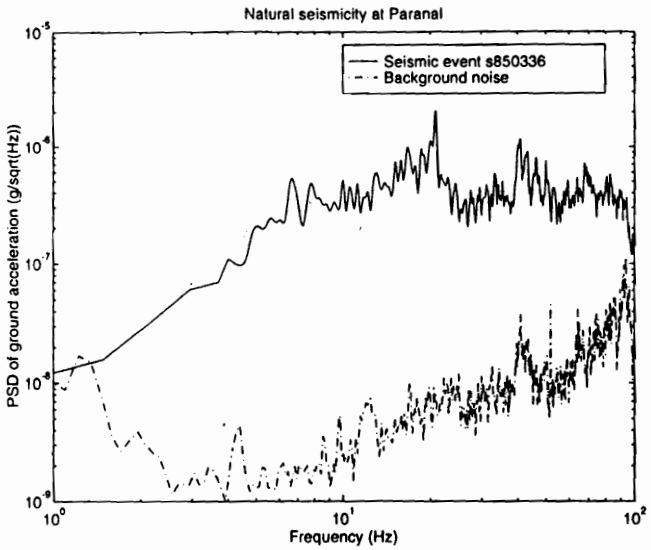

Figure 12: PSD's of ground motion (vertical component) due to natural seismic activity: *Lower:* Background noise in the absence of any artificial disturbance or seismic event, *Upper:* Typical seismic event occuring every 3 hours on average.

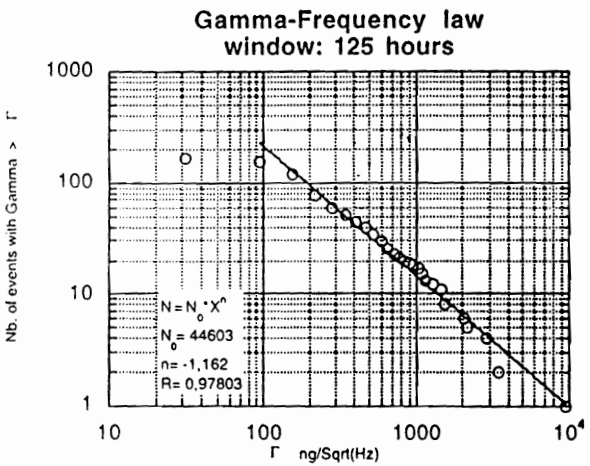

Figure 13: Frequency of occurrence of seismic events at Paranal as characterised by the level of ground acceleration they generate (see text for details).

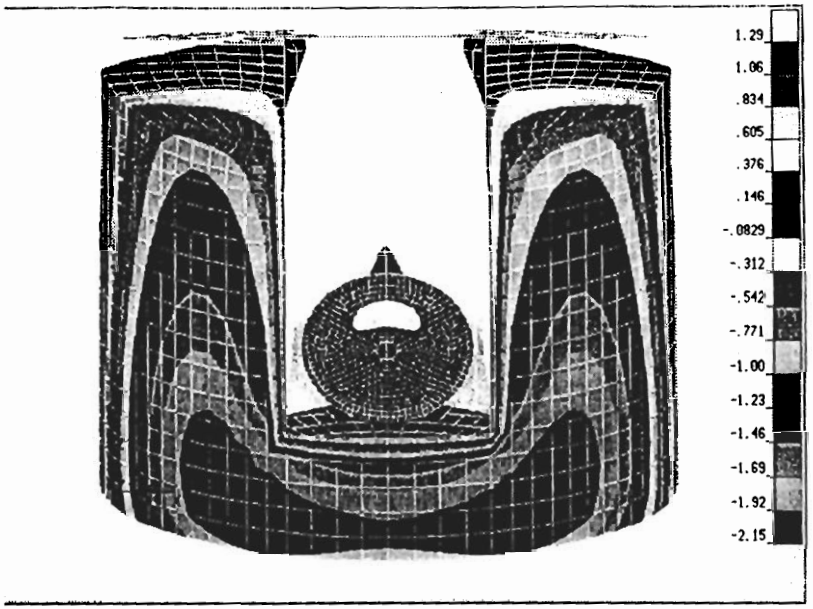

Figure 14: Dynamic acoustic loading (at 13 Hz) on the VLT enclosure and primary mirror due to acoustic noise generated by the interaction of the wind with the entrance slit.

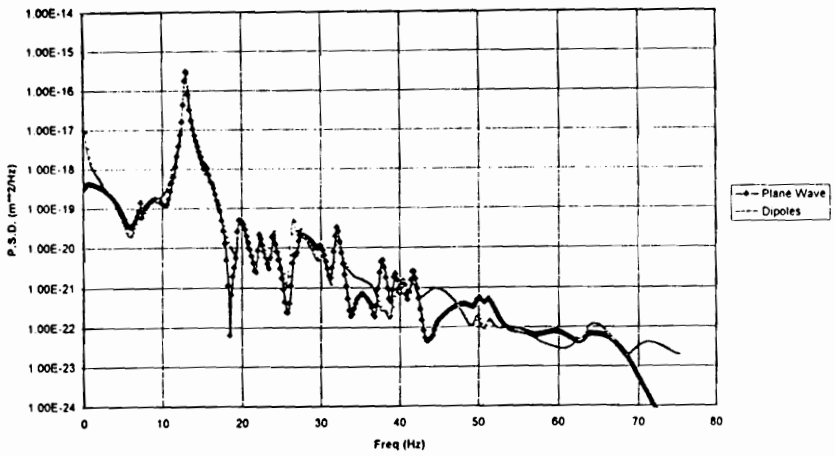

Figure 15: PSD of OPD due to the 8-m primary mirror displacement under acoustic noise generated by the interaction of a 10 m/sec outside wind with the entrance slit.